

Direct observation of the current distribution in thin superconducting strips using magneto-optic imaging

T. H. Johansen, M. Baziljevich, H. Bratsberg, and Y. Galperin
Department of Physics, University of Oslo, P.O. Box 1048, Blindern, 0316 Oslo, Norway

P. E. Lindelof
Niels Bohr Institute, Ørsted Laboratory, Universitetsparken 5, 2100 København Ø, Denmark

Y. Shen and P. Vase
NKT Research Center, Sognvej 11, 2605 Brøndby, Denmark
 (Received 9 July 1996)

Magneto-optic imaging was used for a detailed study of the flux and current distribution of a long thin strip of $\text{YBa}_2\text{Cu}_3\text{O}_{7-\delta}$ placed in a perpendicular external magnetic field. The inverse magnetic problem, i.e., that of deriving from a field map the underlying current distribution, is formulated and solved for the strip geometry. Applying the inversion to the magneto-optically found field map we find on a model-independent basis the current distribution across the strip to be in remarkable agreement with the profile predicted by the Bean model. The paper also presents results on the behavior of the Bi-doped YIG film with in-plane anisotropy which we use as field indicator, explaining why previous measurements of flux density profiles have displayed surprisingly large deviations from the expected behavior. [S0163-1829(96)02046-2]

I. INTRODUCTION

Because of the importance of thin-film applications of high-temperature superconductors there is currently considerable interest in the electric and magnetic properties of such systems. Most experiments with applied magnetic fields are performed in the perpendicular geometry, i.e., with the magnetic field normal to the film plane. Over the last few years several methods have been developed to reveal the spatial distribution of penetrated flux over the area of the sample. Scanning miniature Hall probes, microscopic Hall-sensor arrays, and magneto-optic (MO) imaging have successfully been used to map flux distributions in films and also thin crystals.¹⁻⁸

The results obtained by the field-mapping methods have also stimulated a lot of recent theoretical work aiming to describe the nonuniform and irreversible flux distributions appearing in various two-dimensional (2D) geometries. The simplest case of an infinitely long strip was solved analytically by Brandt *et al.*⁹ and independently by Zeldov *et al.*¹⁰ By assuming a Bean model type of behavior where the current density averaged over the film thickness never exceeds a critical value, and the lower critical field is negligible, they obtained explicit expressions for the field and current distributions across the strip. Also more complicated problems, e.g., by considering shapes like rectangles and circles, have been treated within the framework of the critical-state model in the perpendicular geometry where demagnetization effects are extreme.¹¹⁻¹³

The ultimate goal of any experimental method is to obtain information without involving a physical model for the behavior of the system under study. When it comes to measuring the magnetic field from a quasi-2D or sheet-current distribution it is, in principle, possible to obtain the space-resolved current distribution from a global map of the

perpendicular field component.¹⁴ The model-independent solution of the so-called inverse problem is based only on the Biot-Savart law. Such direct measurement of current distributions have already been reported in studies of superconductors. Xing *et al.*¹⁵ used a scanning Hall probe with a 25 μm resolution to obtain field maps a distance 0.25 mm above a square Y-Ba-Cu-O thin film, and by inversion found current flow patterns in qualitative agreement with a critical-state behavior.

Magnetic-field maps obtained by MO imaging are produced more efficiently and also with a much higher spatial resolution than the scanning Hall technique. In this paper we report on detailed MO studies of a thin superconducting strip in a perpendicular field. For this geometry the inverse problem is solved analytically, where we take into account the fact that the magnetic field is observed a finite distance above the current sheet. This makes the present treatment more general than a previous solution given by Brandt,¹⁶ where the remote nature of these kinds of measurements was neglected. The space-resolved results for the current distribution across the strip are in remarkable agreement with the Bean model prediction, and also demonstrate the powerful application of the MO technique. Also results concerning the behavior of the in-plane MO indicator film are reported.

II. EXPERIMENT

MO visualization of magnetic flux is based on the Faraday effect. In the presence of a magnetic field a Faraday active material will rotate the polarization plane of a linearly polarized transmitted beam of light. The rotation angle increases with the magnitude of the field component parallel to the beam direction and the length of the optical path in the indicator material. Since a superconductor in general will modulate a homogeneous applied field, the response of the

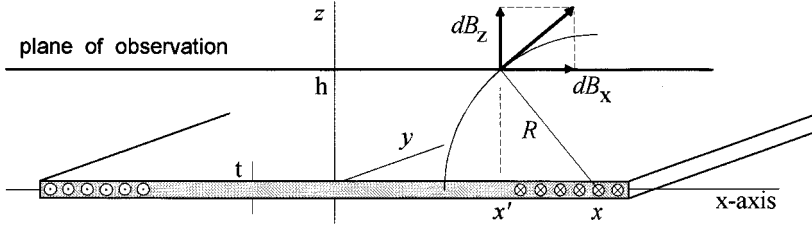


FIG. 1. The geometry of the inversion problem.

superconductor can be directly observed in a polarizing light microscope with crossed polarizers.

A Bi-doped YIG film with in-plane anisotropy was used as the Faraday active indicator.¹⁷ The indicator film was deposited on a gadolinium gallium garnet substrate and covered with a thin reflecting Al layer, allowing for a double pass configuration in our incident-light microscope. The images were recorded with an eight-bit Kodak DCS 420 CCD camera and transferred to a computer for processing.

Thin films of $\text{YBa}_2\text{Cu}_3\text{O}_{7-\delta}$ were made by laser ablation on a (100) SrTiO_3 substrate. A deposition pressure of 1 mbar and a substrate temperature of 750 °C were used. More details of the preparation can be found in Ref. 18. The sample used in the present work has a thickness of $t=300$ nm with the c axis oriented perpendicular to the film plane. The lateral shape of the film was formed by etching resulting in a 5 mm long rectangular strip with a half width of $a=0.4$ mm. The critical temperature, T_c measured by magnetic susceptibility was 89.9 K with $\Delta T_c=0.3$ K. In the MO apparatus the sample was mounted on the cold finger of an optical Helium cryostat.¹⁹ The magnetic field was applied perpendicular to the film plane using a Cu-wire solenoid.

III. THE 1D INVERSION PROBLEM

As the aim of this work was to determine the current distribution from a map of the magnetic field we give here the solution to the appropriate inversion problem. Consider a current flowing in a planar sheet of thickness t lying in the x - y plane; see Fig. 1. We assume that the current is directed along the y axis producing a B field in the x - z plane. If the current sheet is thin compared to the distance to the plane of observation, i.e., $t \ll h$, the current distribution can be treated as one dimensional and described by a sheet current $J(x) = \int_0^t j(x, z) dz$, where $j(x, z)$ is the local current density.

From the law of Biot-Savart the contribution to the perpendicular field component at the point x' from the current element $J(x)dx$ is

$$dB_z = \frac{\mu_0}{2\pi} \frac{J(x)dx}{R} \frac{x-x'}{R}, \quad (1)$$

where $R = \sqrt{h^2 + (x-x')^2}$. Integrating over all the current filaments the total perpendicular field profile can be expressed as

$$B_z(x') = \frac{\mu_0}{2\pi} \int_{-\infty}^{\infty} \frac{x-x'}{h^2 + (x-x')^2} J(x) dx. \quad (2)$$

This convolution form allows us to write the current as

$$\mu_0 J(x) = \int_{-\infty}^{\infty} \frac{B_z(k)}{G(k)} e^{ikx} dk, \quad (3)$$

where $B_z(k)$ and $G(k)$ are the Fourier transforms of the field profile and integral kernel, respectively. The function $G(k)$ equals

$$G(k) = \int_{-\infty}^{\infty} \frac{P}{h^2 + p^2} e^{-ikp} dp = -i\pi \operatorname{sgn}(k) e^{-h|k|}. \quad (4)$$

It is seen from Eqs. (3) and (4) that the transfer function $1/G(k)$ strongly amplifies components in the B_z signal with large $|k|$ values. On the other hand, it is likely that in the experimentally obtained B_z data the components with highest $|k|$ originate from other sources than the currents in the sample. For this reason one would like to include a low-pass filter in the signal analysis. Assuming that the filter cuts the components with $|k| \geq K$ we rewrite Eq. (3) as

$$\mu_0 J(x) = \int_{-\infty}^{\infty} dx' A(x-x') B_z(x'), \quad (5)$$

$$A(\xi) = \int_{-K}^K dk \frac{e^{ik\xi}}{G(k)} = \frac{\xi [1 - e^{Kh} \cos K\xi] + h e^{Kh} \sin K\xi}{h^2 + \xi^2}.$$

For the computerized data analysis it is convenient to introduce the unit of length $\Delta \equiv \pi/K$ and to discretize the coordinates, $x \equiv n\Delta$, $x' \equiv n'\Delta$, and also write $h \equiv d\Delta$. For the ideal low-pass filter Eq. (5) becomes

$$\mu_0 J(n) = \sum_{n'} \frac{n-n'}{d^2 + (n-n')^2} \frac{1 - (-1)^{n-n'} e^{\pi d}}{\pi} 2B_z(n'). \quad (6)$$

A smoother high-frequency cutoff is obtained by introducing in Eq. (3) a Hanning window filtering function

$$W(k) = [1 + \cos(\pi k/K)]/2 \quad \text{for } |k| \leq K,$$

with $W(k)=0$ for $|k| > K$. This modifies only slightly the derivation, and the inversion formula now becomes

$$\mu_0 J(n) = \sum_{n'} \frac{n-n'}{\pi} \left\{ \frac{1 - (-1)^{n-n'} e^{\pi d}}{d^2 + (n-n')^2} + \frac{[d^2 + (n-n')^2 - 1][1 + (-1)^{n-n'} e^{\pi d}]}{[d^2 + (n-n'+1)^2][d^2 + (n-n'-1)^2]} \right\} \times B_z(n'). \quad (7)$$

In the Appendix the use of the inversion method is illustrated by an exactly solvable example.

IV. RESULTS FOR THE SUPERCONDUCTING STRIP

The MO image shown in Fig. 2 was obtained at $T=10$ K by applying an external field of $B_a=40$ mT to the zero-field cooled superconductor. Its shielding property is evident as the field becomes compressed near the strip edge (maximum brightness). The outmost part of the strip is seen to be penetrated by flux lines with a distribution which gives rise to the gradual decrease in the gray level towards the center. The dark and uniform central area corresponds to the Meissner region where the induced sheet current exactly compensates for the applied field.

Figure 3 shows the observed flux density profile across the strip. The data points were obtained by converting the gray levels of the image into B_z values along a line indicated in Fig. 2. The conversion is based on a careful calibration of the Bi:YIG indicator response to a range of controlled perpendicular magnetic fields as seen by the CCD camera through the microscope. Figure 4 shows the current distribution obtained by inverting the field data of Fig. 3. Note that the inversion procedure requires that the applied field is subtracted from the B_z data. The current was calculated using Eq. (7) setting $d=1.5$, which corresponds to $h=10$ μm .

Both results agree reasonably well with the behavior predicted by the Bean model applied to the present transverse geometry. The analytical solution for an infinitely long strip of half-width a is

$$J = \begin{cases} J_c, & -a < x \leq -x_p \\ -\frac{2J_c}{\pi} \tan^{-1} \left(\frac{x}{a} \sqrt{\frac{a^2 - x_p^2}{x_p^2 - x^2}} \right), & -x_p < x < x_p \\ -J_c, & x_p \leq x < a, \end{cases} \quad (8)$$

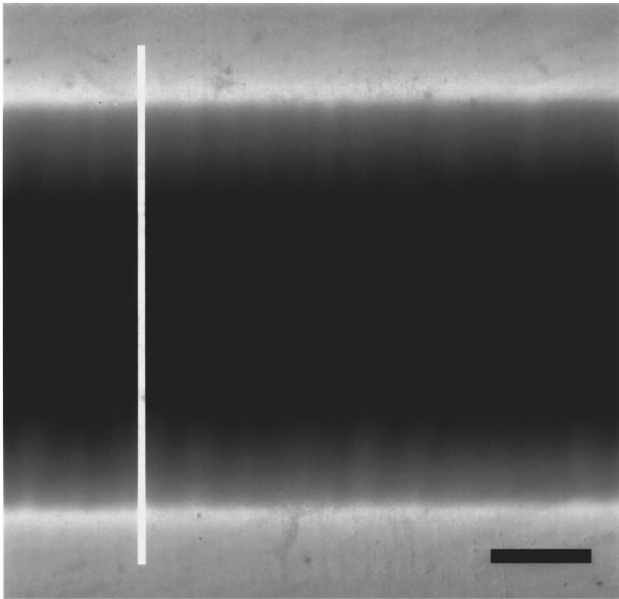


FIG. 2. Magneto-optic image of the flux penetration in a 0.8 mm wide, 300 nm thick, and 5 mm long Y-Ba-Cu-O strip placed in a 40 mT perpendicular applied field at 10 K. The section shown in the picture was chosen near the central part of the strip where the influence of the corners is negligible. The white line indicates where the profile of Fig. 3 was measured. The scale bar is 0.2 mm long.

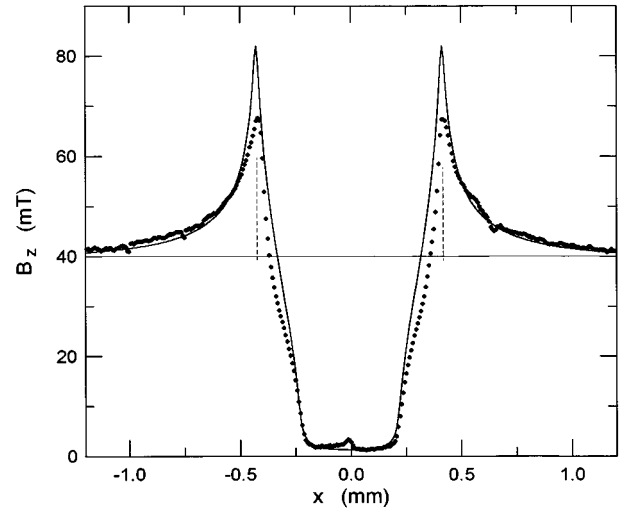


FIG. 3. Measured and calculated perpendicular flux density profile along a line across the Y-Ba-Cu-O strip (cf. Fig. 2). The dashed lines indicate the position of the strip edges.

where

$$x_p = \frac{a}{\cosh(\pi B_a / \mu_0 J_c)}$$

is the position of the flux penetration front and J_c is the critical sheet current. According to the Biot-Savart law the current distribution described by Eq. (8) gives in a distance h the following B_z profile:

$$B_z(x) = \frac{\mu_0 J_c}{4\pi} \left\{ \ln \frac{[(x+x_p)^2 + h^2][(x-x_p)^2 + h^2]}{[(x+a)^2 + h^2][(x-a)^2 + h^2]} - \frac{4}{\pi} \int_{-x_p}^{x_p} \frac{x' - x}{(x' - x)^2 + h^2} \times \tan^{-1} \left(\frac{x'}{a} \sqrt{\frac{a^2 - x_p^2}{x_p^2 - x'^2}} \right) dx' \right\}. \quad (9)$$

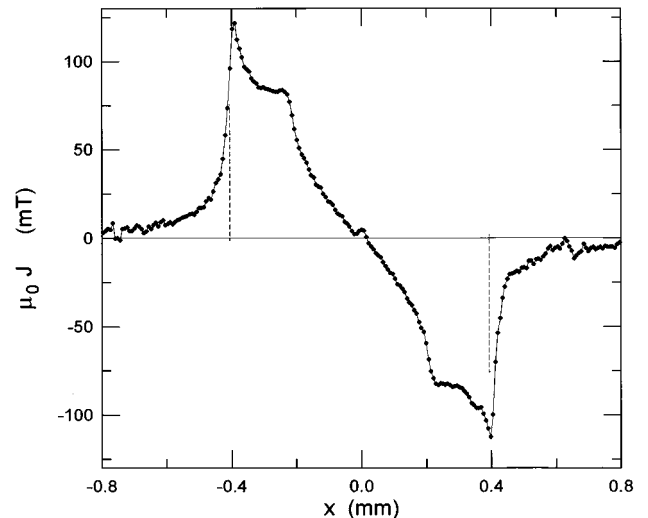


FIG. 4. The sheet current distribution obtained by applying the inversion formula Eq. (7) to the B_z data of Fig. 3.

For comparison, the field profile plot includes a fit of the Bean model which gave $\mu_0 J_c = 105$ mT, or a critical current density of 2.8×10^{11} A/m².

While the overall agreement with the Bean model is reasonable there are also several distinct discrepancies apparent from the curves. In the experimental B_z data the U-shaped part of the profile is evidently too wide. Moreover, the peaks near the edges of the strip are much lower than expected. Interestingly, the same types of deviation can be seen also in other MO investigations of thin superconducting strips.²⁰ A common systematic error seems to be that the experimental B_z profiles violate the requirement of a vanishing integral of the flux density. Also in the inferred current distribution there are clear discrepancies. Most serious is the unphysical result that $J \neq 0$ outside the strip. Unexpected is also the sharp increase in J towards the two edges.

Puzzled by these deviations we critically investigated possible sources for misinterpretation of the MO images. In this search we discovered that the Bi:YIG indicator not only responds to B_z , but is also influenced by a field component B_x parallel to the film. Although the present experiments were performed with a perpendicular applied field, it is clear that the shielding currents in the superconductor produce a considerable parallel field in the plane of the indicator. This, so far unreported MO coupling, will be discussed in more detail in the next section.

V. THE B_x COUPLING

To investigate the role of a parallel magnetic field on the Faraday rotation in the MO indicator the optical cryostat was equipped with an additional field source. A variable parallel field was produced by adjusting the separation between a pair of strong permanent magnets placed on the outside of the standard B_z solenoid. A calibration of the CCD image gray level versus perpendicular field, B_z , was made for three different B_x values; see Fig. 5. The measurements were done with the MO indicator at $T=50$ K, and with the supercon-

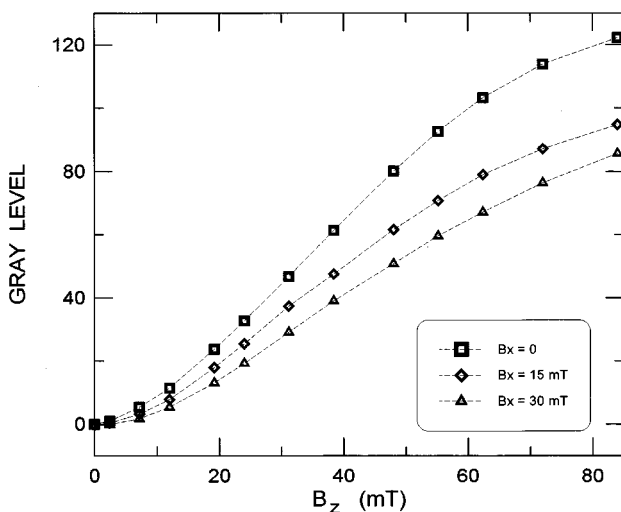


FIG. 5. The gray level output of the CCD camera as function of the perpendicular magnetic field, B_z , applied to the Bi:YIG indicator film. The three different graphs were obtained by adding a parallel field component B_x equal to 0, 15, and 30 mT.

ductor removed. It is clear from the graphs that even moderate parallel fields give a significant reduction in the gray level, or equivalently a reduced Faraday rotation angle θ_F . The behavior can be explained as follows.

The MO indicator material is ferrimagnetic having a spontaneous magnetization, \mathbf{M}_s , with the easy axis lying in the film plane. A magnetic field \mathbf{B} at an angle α (see Fig. 6) will force the magnetization vector out of the plane. The equilibrium tilt angle ϕ of the magnetization represents the balance between the magnetocrystalline anisotropy and the tendency to align with the external field. In the simplest form this can be expressed as a minimum of the sum

$$E_A(1 - \cos\phi) + BM_s[1 - \cos(\alpha - \phi)], \quad (10)$$

where E_A is the anisotropy energy. Minimizing the above energy expression with respect to the variable angle ϕ one finds

$$\tan\phi = \frac{B_z}{B_A + B_x}, \quad (11)$$

where $B_A = E_A/M_s$. As the Faraday rotation is proportional to the component of \mathbf{M}_s along the light beam direction it follows that

$$\theta_F \propto \sin\phi = \frac{B_z}{\sqrt{(B_A + B_x)^2 + B_z^2}}. \quad (12)$$

This model describes both the observed suppression of θ_F by a parallel field and also the saturation seen for large B_z .

VI. DISCUSSION

Having now available a realistic model for the response of the indicator film it is possible to take the effect of a parallel field into account when MO images are interpreted. To accomplish this a quantitative determination of the anisotropy field B_A is required. The following analysis allowed us to derive this parameter from the calibration data.

From the Malus law for light transmission through a pair of polarizers the light intensity reaching the CCD chip is $I \propto \sin^2\theta_F$ in the case of crossed polarizers. The CCD camera then converts the light intensity into gray level values, G . Linearizing this camera function in the small intensity range implies $G \propto \sin^2\theta_F \approx \theta_F^2$. From Eq. (12) it then follows that

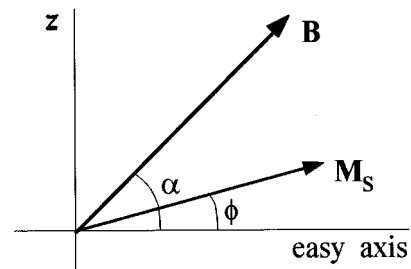


FIG. 6. Relation between the directions of the spontaneous magnetization \mathbf{M}_s of the in-plane indicator film and the magnetic field \mathbf{B} , which forces the magnetization vector away from the easy axis.

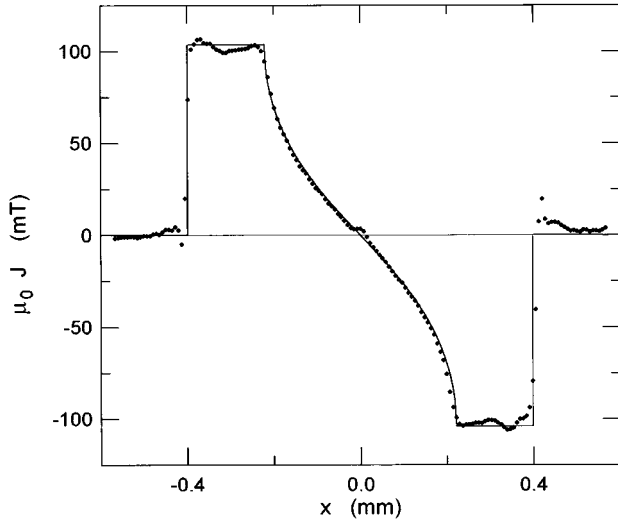


FIG. 7. The sheet current distribution in the Y-Ba-Cu-O strip obtained from the MO image by a modified inversion procedure (see text). For comparison, the theoretical curve following from the Bean model with $\mu_0 J_c = 105$ mT is drawn as a full line.

$$G \propto \frac{1}{(B_A + B_x)^2} B_z^2. \quad (13)$$

Such a parabolic dependence is indeed representative for the observed behavior in the limit of small fields. A fit of this relation to the initial part of the curves in Fig. 5 gave $B_A = (80 \pm 5)$ mT.

The recalculated current distribution shown in Fig. 7 was found using a modified inversion procedure. From Eq. (12) and the unique, although unknown, relationship between G and θ_F , it follows that B_z can be expressed by $B_z = (B_A + B_x)f(G)$ where f is some function. Note here that B_z and B_x are the total fields experienced by the indicator film, i.e., the perpendicular field due to the current alone is $B_z^J = (B_A + B_x)f(G) - B_A$. Since the initially obtained $J(x)$ was close to the expected distribution an approximate B_x profile is derived from the Biot-Savart law applied to the initial $J(x)$ where the unphysical current tail outside the strip is removed by hand. A new B_z^J is then obtained from

$$B_z^J(\text{new}) = B_z^J(\text{old}) + \frac{B_x}{B_A} B_z(\text{old}). \quad (14)$$

The current distribution of Fig. 7 results from inverting B_z^J (new).

Included in Fig. 7 is also the theoretical curve given by Eq. (8) with, as before, $\mu_0 J_c = 105$ mT. As our data for the current were obtained independently of any model for the superconductor the excellent fit gives direct evidence for the validity of the critical-state assumptions made in the Bean model. Note in particular that the inversion can provide information about the Meissner current distribution; the S-shaped part of the curve in the middle part of the strip. Information about the Meissner current flow is not easily inferred from maps of the magnetic field since the Meissner region always appears without any structure. Only an analysis based on the global field distribution, as in the inversion described in this work, is able to accomplish this.

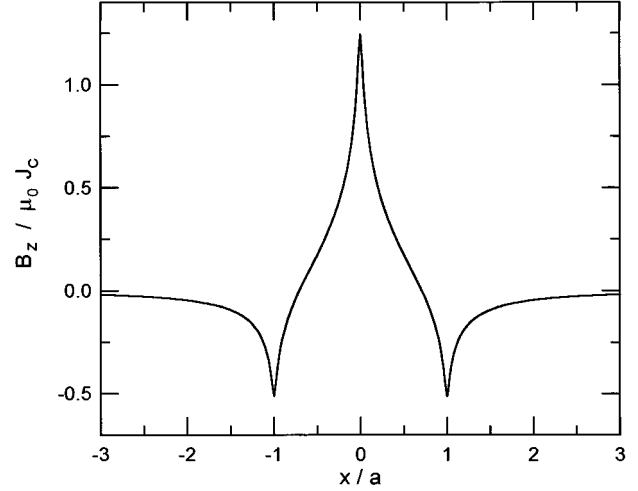


FIG. 8. Profile of the perpendicular magnetic field across a strip of sheet current with magnitude $-J_c$ and $+J_c$ flowing in each half of the strip.

VII. CONCLUSION

In this paper we considered the possibility of inverting magnetic-field maps to give direct observations of current distributions in thin superconducting samples. Choosing the simplest geometry, i.e., that of a long thin strip, allowed us to investigate this issue in great detail. Our model-independent results for the current distribution across the strip shows that the Bean model gives an excellent description.

A by-product of the investigation was to discover that MO images are significantly perturbed by the presence of a parallel field component. A simple model for the behavior of the Bi-doped YIG indicator film with in-plane anisotropy was shown to give a realistic description of the film response. The model also explains why previous measurements of flux density profiles have displayed surprisingly large deviations from the expected behavior. We believe this work represents an important step towards bringing the MO imaging method to a more precise quantitative level.

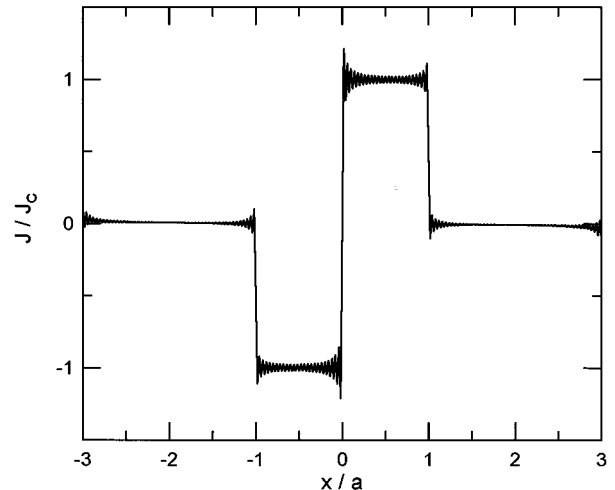


FIG. 9. Sheet current density derived by inversion of the field profile in Fig. 8 using Eq. (6) in Sec. III.

ACKNOWLEDGMENT

This work was financially supported by The Norwegian Research Council.

APPENDIX

In contrast to the forward calculation of the magnetic field produced by some current distribution $\mathbf{J}(\mathbf{r})$, the inverse problem does not, in general, have a unique solution. However, when the current is restricted to flow in a planar sheet the inverse problem can be solved uniquely. To verify the applicability of the inversion formulas derived in Sec. III we give here a transparent example.

Consider the infinitely long strip of half-width a in the configuration shown previously in Fig. 1. Assume now that a current of a constant magnitude $-J_c$ flows in the half $-a \leq x < 0$, whereas $+J_c$ flows in the other half $0 < x \leq a$. For superconductors this corresponds to the state of complete flux penetration within the critical-state model. It is readily found that the perpendicular magnetic field a distance h above the strip is given by

$$B_z(x) = -\frac{\mu_0 J_c}{4\pi} \ln \frac{(x^2 + h^2)^2}{[(x+a)^2 + h^2][(x-a)^2 + h^2]}. \quad (\text{A1})$$

The field profile is shown in Fig. 8 for the case $h/a = 1/40$.

Applying the inversion formula, Eq. (6), with the discretization $\Delta = h$, or $d = 1$, one obtains the result shown in Fig. 9. Evidently, the correct current profile is restored, although with the addition of some high-frequency oscillations near the points where the current changes discontinuously. Such alternating noise decreases rapidly in amplitude when d becomes less than unity, while a strong noise enhancement results if d exceeds unity. In the calculation this is a direct

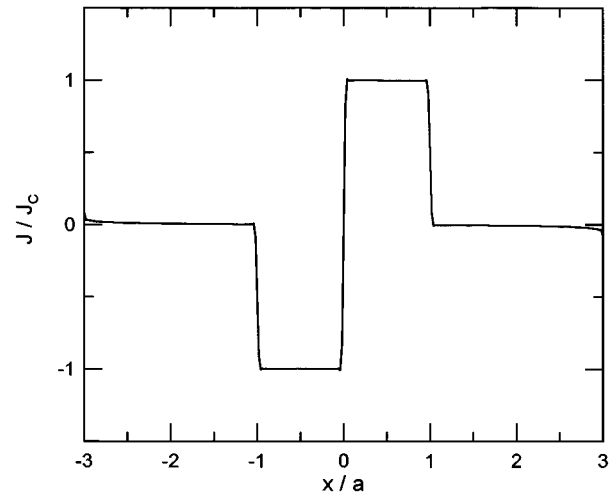


FIG. 10. Sheet current density derived by inversion of the field profile in Fig. 8 using Eq. (7) in Sec. III.

consequence of the exponential term $e^{\pi d}$ becoming very large. Physically, it signals the failure of retrieving the fine details in the current distribution out of a field distribution smeared because of the remote observation.

The alternating noise problem is overcome by the Hanning window low-pass filtering leading to Eq. (7). As seen in Fig. 10 the original current distribution now becomes reconstructed almost exactly from the discrete set of B_z data.

Note that the inversion formula requires that B_z used in the calculation corresponds to the field from the current only. Any applied field contained in the field profile should therefore be subtracted. It is also important that the B_z data cover a sufficiently wide area so that the clipping of the tail of the field has no significance for the result.

¹P. Brüll *et al.*, Physica C **182**, 339 (1991).

²W. Rauch *et al.*, Physica C **201**, 179 (1992).

³E. Zeldov *et al.*, Europhys. Lett. **30**, 367 (1995).

⁴M. R. Koblischka and Wijngaarden, Supercond. Sci. Technol. **8**, 199 (1995).

⁵R. Knorpp *et al.*, Physica C **230**, 128 (1994).

⁶M. V. Indenbom *et al.*, Physica C **209**, 259 (1993).

⁷V. K. Vlasko-Vlasov *et al.*, Physica C **222**, 361 (1994).

⁸M. Baziljevich *et al.*, Physica C **266**, 127 (1996).

⁹E. H. Brandt *et al.*, Europhys. Lett. **22**, 735 (1993).

¹⁰E. Zeldov *et al.*, Phys. Rev. B **49**, 9802 (1994).

¹¹E. H. Brandt, Phys. Rev. B **49**, 9024 (1994).

¹²E. H. Brandt, Phys. Rev. B **50**, 4034 (1994).

¹³E. H. Brandt, Phys. Rev. B **52**, 15 442 (1995).

¹⁴B. J. Roth *et al.*, J. Appl. Phys. **65**, 361 (1989).

¹⁵W. Xing *et al.*, J. Appl. Phys. **76**, 4244 (1994).

¹⁶E. H. Brandt, Phys. Rev. B **46**, 8628 (1992).

¹⁷L. A. Dorosinskii *et al.*, Physica C **203**, 149 (1992).

¹⁸P. Vase *et al.*, Physica C **180**, 90 (1991).

¹⁹M. V. Indenbom *et al.*, Physica C **166**, 486 (1990).

²⁰See, e.g., Th. Schuster *et al.*, Phys. Rev. B **50**, 16 684 (1994).